Article

Adsorption by Granular Activated Carbon and Nano Zerovalent Iron from Wastewater: A Study on Removal of Selenomethionine and Selenocysteine

Stanley Onyinye Okonji [1], **Linlong Yu** [2], **John Albino Dominic** [2], **David Pernitsky** [3] **and Gopal Achari** [2,*]

[1] Department of Mechanical & Manufacturing Engineering, University of Calgary, ICT 402, 2500 University Drive NW, Calgary, AB T2N 1N4, Canada; stanley.okonji@ucalgary.ca

[2] Department of Civil Engineering, University of Calgary, ENF 262, 2500 University Drive NW, Calgary, AB T2N 1N4, Canada; linyu@ucalgary.ca (L.Y.); johnalbino.dominic@ucalgary.ca (J.A.D.)

[3] Stantec, 200-325 25 Street SE, Calgary, AB T2A 7H8, Canada; David.Pernitsky@stantec.com

* Correspondence: gachari@ucalgary.ca

Abstract: Selenomethionine (SeMet) and selenocysteine (SeCys) are the most common forms of organic selenium, which is often found in the effluent of industrial wastewater. These organic selenium compounds are toxic, bioavailable and most likely to bioaccumulate in aquatic organisms. This study investigated the use of two adsorbent candidates (granular activated carbon (GAC) and nano zerovalent iron (nZVI)) as treatment technologies for SeMet and SeCys removal. Batch experiments were performed and inductively coupled plasma optical emission spectrometer (ICP-OES) was used for sample analysis. Experimental data showed GAC demonstrated a higher affinity towards the removal of SeMet and SeCys compared to nZVI. The removal efficiency of SeCys and SeMet by GAC was 96.1% and 86.7%, respectively. NZVI adsorption capacity for SeCys was 39.4% and SeMet < 1.1%. Irrespective of the adsorbent, SeMet is more refractory to be adsorbed compared to SeCys. Kinetics data of GAC and nZVI agreed well with the pseudo-second-order model ($R^2 > 0.990$). The experimental data of SeCys was characterized by Langmuir model, indicating monolayer adsorption. The adsorption capacity of nZVI for SeCys increased significantly by about 35%, with a decrease in pH from 9.0 to 4.0, indicating that SeCy removal by nZVI is pH dependent. While electrostatic attraction is considered the driving mechanism for nZVI adsorption, GAC uptake capacity is controlled by weak van der Waal forces. The adsorption of binary adsorbates (SeMet and SeCys) exhibited an inhibitory effect due to the competitive interaction between contaminant molecules.

Keywords: adsorption; nano zerovalent iron; granular activated carbon; organoselenium; water; wastewater; treatment

1. Introduction

Organoselenium simply refers to compounds that contain selenium (Se) in combination with other elements, such as carbon, oxygen, hydrogen, and nitrogen as part of their structure. The primary form of organic Se is selenoamino acids and selenoproteins [1]. SeMet and SeCys are the most common forms by which Se-amino acids exist in the environment and are uptaken by plants and aquatic organisms [2,3]. Naturally, SeMet and SeCys are organically bound in foods, such as nuts, yeast, eggs, liver, garlic [1,3]. In general, Se is a trace element essential for living organism physiological processes at a concentration range from 63–135 µg/L but exhibits toxicity outside this range of concentration [4].

In aqueous environments, organic selenium can be categorized as an emerging contaminant. It exists in the form of SeMet and SeCys in the effluent of industrial wastewaters [5], emanating from mostly mining, oil and gas refineries and coal-fired power plants. SeMet and SeCys are known to have higher bioavailability than inorganic selenium species as it is readily absorbed [3,5]. As a result, the ecotoxicological effect of organic Se (SeMet

and SeCys) in aqueous environments is increased. One of the major concerns of organic selenium is the tendency to accumulate in aquatic organisms for an extended period of time, resulting in the contamination of fish and wildlife diets [6]. Public health is at risk if humans consume selenium-contaminated fish and wildlife [7]. The US EPA recently set environmental Se threshold regulations to be reliant on biotic tissue-based concentration rather than the traditional aqueous concentration limit [8]. This regulation is key to preventing organic Se propensity to bioaccumulate within the food-web. Therefore, it is essential to remove organic selenium contaminants from industrial wastewaters in order to decrease the bioaccumulation of selenium in aquatic life, the adverse impact on the ecosystem and the threat to public health. However, there are limited options available for the industries to meet this regulation.

To date, research on selenium remediation in aqueous media has largely focused on inorganic selenium removal. Various treatment technologies have been explored to remove Se from industrial wastewater. These are broadly classified into physical, chemical and biological treatment processes [9,10]. The following studies investigated these removal technologies: elemental selenium (Se^0) precipitation [11,12], iron coprecipitation methods [13], ion-exchange [14], adsorption using mineral adsorbents [15–21], coagulation [22], electrocoagulation [14] and photocatalytic reduction [23,24]. The biological treatment method is the most commonly used remediation technology for inorganic Se removal [10]. The process relies on the use of microbial mediation for selenium species removal [25–28]. However, the presence of SeMet has been reported in the effluents of an industrial biological treatment system [5]. It stands to reason that biological treatment techniques are among the primary sources of organic Se pollution in wastewaters. The transformation of inorganic selenium species to the organic form is mainly due to the microbial activities [5,29]. As a result, the existence of organic Se (SeMet and SeCys) in wastewaters remains an environmental contaminant of concern and the remediation techniques have rarely been researched.

So far, very few studies had investigated organic selenium removal from wastewaters. Alain (1997) investigated the removal of selenocyanate ($SeCN^-$) from sour crude oil produced wastewater by copper (II) salt precipitation [30]. Meng 2002 [31] studied the removal of selenocyanate ($SeCN^-$) from wastewater using Fe(0) filings through the formation of elemental selenium (Se^0). Sanna (2003) studied seleno-DL-methionine separation from inorganic selenium solution using magnesium-loaded activated charcoal [32]. However, besides our earlier study on SeMet removal [33], no previous research has investigated the removal of SeMet and SeCys from wastewater.

This study was conducted to determine the removal of SeMet and SeCys from wastewaters by (granular activated carbon (GAC) and nano zerovalent iron (nZVI)) adsorption, which have shown promise in treating inorganic selenium [34–36]. In this research, adsorption kinetics and isotherms of the two adsorbents were investigated. The effects of pH, initial adsorbate concentrations on adsorption capacities and the influence of binary adsorption were evaluated. SeMet and SeCys were selected as probe contaminants due to its toxicity and bioavailability in the wastewater, while the choice of adsorbents was driven by inexpensive cost and their being environmental benign [37,38]. This is the first study investigating the mechanism of GAC and nZVI to remove organic selenium from industrial wastewater. The knowledge gain in this study will benefit the development of efficient treatment processes for SeMet and SeCys using GAC and nZVI.

2. Materials and Methods

2.1. Chemicals

All chemicals employed in this study were used as received. Selenomethionine (>98%) and selenocysteine (>98%) were purchased from TCI America. Hydrochloric acid (HCl) (>98%), sodium hydroxide (NaOH) (>98%), nano zerovalent iron (nZVI 60–80 nm >99%) were procured from Sigma-Aldrich Chemical Company. Granular activated carbon was acquired from Evoqua (Pittsburgh).

2.2. Characterization of Adsorbents

The morphological properties of the adsorbents were obtained on a scanning electron microscope (SEM, ThermoFisher, Quanta FEG 250), as shown in Figure 1. BET surface area and total pore volume were obtained by N_2 adsorption at 77 K on a PMI Automated Brunauer–Emmett–Teller (BET), Quantachrome ChemBet (3000 CB-SCL).
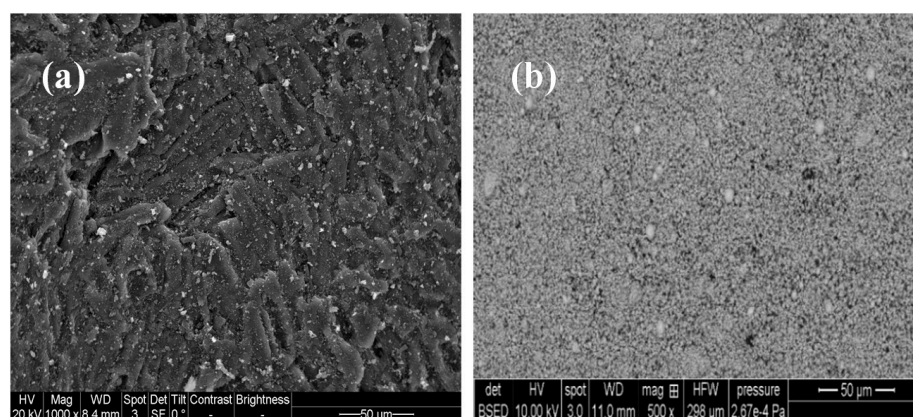

Figure 1. SEM images of granular activated carbon (**a**) and nZVI (**b**).

2.3. Batch Adsorption Studies

Selenocysteine ($C_3H_7NO_2Se$) and Selenomethionine ($C_5H_{11}NO_2Se$) stock solution were prepared separately by dissolving 0.5 g of both compounds in 100 mL of deionized water. The stock solution was diluted appropriately to obtain working solutions of various concentrations, as needed. The concentration of SeMet and SeCys in working solutions, used for adsorbent dose studies, pH studies, initial adsorbate concentrations and adsorption kinetics, was 5 mg/L. Table 1 illustrates the summary of experimental conditions with respect to the adsorbents and their respective concentrations used for evaluating adsorbent dose studies. The effect of pH on the adsorption of SeMet and SeCys was investigated by conducting experiments with different pH conditions (4.0, 7.0 and 9.0). Batch experiments were performed using straight-wall glass jars of 150 mL volume. A magnetic stirrer (VWR 200 model) was used to stir the solutions; the mixtures was agitated at a constant shaking speed of 180 rpm in a temperature-controlled orbital shaker. All experiments were conducted at ambient temperature. The initial pH of the solution was adjusted by adding HCl or NaOH (1 M). At different time intervals, aliquots of 10 mL samples were periodically taken and immediately filtered using 0.22 μm PTFE syringe filter. The collected samples were acidified using 50% nitric acid for a resulting strength of 2% and stored at 4 °C before analysis. For statistical reliability, all the experiments were conducted in duplicate, the samples were analyzed in triplicate and standard deviation was used for error analysis.

Table 1. Summary of experimental conditions for adsorbent dose.

	SeCys		SeMet	
Adsorbent Type	**GAC**	**nZVI**	**GAC**	**nZVI**
	1	-	1	-
	2	2	2	-
Dosage (g/L)	3	-	3	-
	5	-	5	-
	7	7	7	7
	14	14	14	-

2.4. Analysis and Equipment

The total Se concentration in the samples was analyzed using an inductively coupled plasma optical emission spectrometer (ICP-OES) (Thermo Scientific icap 7000 series). The limit of detection and quantitation for selenium was estimated as 0.005 and 0.01 mg/L, respectively. The pH fluctuations in the system with time were measured with a pH digital instrument symphony B20PI VWR. The analysis in this study did not distinguish between the species of organic selenium. The total selenium concentration was measured and analyzed.

2.5. Adsorption Kinetics

Adsorption kinetics were examined for an SeMet and SeCys initial concentration of 5 mg/L using nZVI and GAC adsorbent. An adsorbent loading rate of 7 g/L was used and the adsorption capacity q_e (mg/g) was calculated using the expression (Equation (1)):

$$q_e = \frac{C_o - C_e}{M} V \tag{1}$$

where C_o and C_e represent initial and equilibrium concentrations (mg/L), respectively; M is the mass of the adsorbent (g); V is the volume of the solution (L). A pseudo-second-order kinetic model was applied to the kinetic data; the mathematical expression is shown in Equation (2):

$$\frac{t}{q_t} = \frac{1}{k_2 q_e^2} + \frac{t}{q_e} \tag{2}$$

where q_e and q_t (mg/g) represent the amount of adsorbate adsorbed at equilibrium and time (t), respectively; k_2 is pseudo-second-order kinetic rate constant (g·mg^{-1}min^{-1}) and adsorption time (min). The initial adsorption rate h of the system is equal to $k_2 q_e^2$ (mg·g^{-1} min^{-1}). Equation (3) shows the pseudo-first-order kinetic model:

$$q_t = q_e \left(1 - e^{-kt} \right) \tag{3}$$

where k (min^{-1}) is the rate constant; other parameters in the expression have been defined above.

2.6. Adsorption Isotherm Studies

Adsorption isotherm studies were conducted with various initial concentrations (5 to 47.2 mg/L) for SeMet and SeCys. Freundlich and Langmuir isotherm models were used to evaluate the adsorption isotherm. The Freundlich model describes the relationship between the equilibrium concentration and the adsorption capacity. Equation (4) describes the nonlinear Freundlich adsorption isotherm model [39]:

$$\frac{(C_o - C_e)}{M} V = K_f C_e^{\frac{1}{n}} \tag{4}$$

where C_e is the equilibrium concentration (mg/L), C_o is the initial concentration (mg/L), M is the mass of adsorbent (g), V is the volume of the solution (L), K_f and n are Freundlich constants. The left-hand side of the Equation can be determined from experimental data, and it denotes the mass of adsorbate adsorbed per unit mass of adsorbent. The mathematical expression of Langmuir isotherm model [40] is given in Equation (5):

$$q_e = q_m K_c \frac{C_e}{1 + K_c C_e} \tag{5}$$

where q_e is the adsorption capacity at equilibrium (mgSe/g), q_m (mgSe/g) is the maximum adsorption capacity, K_c (L/mg) defined the equilibrium adsorption constants and C_e is the equilibrium concentration (mg/L). The Langmuir isotherm is based on the assumption

that adsorption can occur at a finite number of specific localized sites (monolayer) [40]. Equation (6) can be used to evaluate the Langmuir model further [41].

$$R_L = \frac{1}{1 + K_c C_o} \tag{6}$$

The value of R_L defines the adsorption process as irreversible when ($R_L = 0$), favorable ($1 > R_L > 0$), unfavorable ($R_L > 1$) and linear ($R_L = 1$).

2.7. Parameter Study

The impact of various parameters, including adsorbent dose, pH and initial adsorbate concentration on organic selenium adsorption were evaluated. The experimental conditions were described in Section 2.3 and are summarized in Table 1 (adsorbent dose). The adsorbent amount of 7 g/L was chosen for all experiments based on the optimum dose determined in the dosage studies. For the binary adsorption experiment, a solution containing a mixture of SeMet and SeCys was used to study the effect of organic selenium coexistence. The initial concentration of the organoselenium was 5 mg/L each.

3. Results and Discussion

3.1. Adsorption of Organic Selenium by nZVI and GAC

The batch experiments result for the adsorption of organic selenium species (SeMet and SeCys) using 7 g/L of nZVI and GAC are presented in Figure 2. As shown, the removal of SeCys and SeMet by GAC is more effective than nZVI. After 3 h of adsorption experiments, it was observed that 96% of SeCys and 86.76% of SeMet was removed from water by activated carbon, while 39.44% of SeCys and less than 1.05% of SeMet was transferred to nZVI from the aqueous phase. Physisorption and chemisorption are the two major mechanisms for activated carbon adsorption. The former is caused by relatively weak van der Waals forces formed between the adsorbates and activated carbon's surface. In contrast, the latter is driven by a chemical reaction between the adsorbate molecules and the adsorbent surface [42].
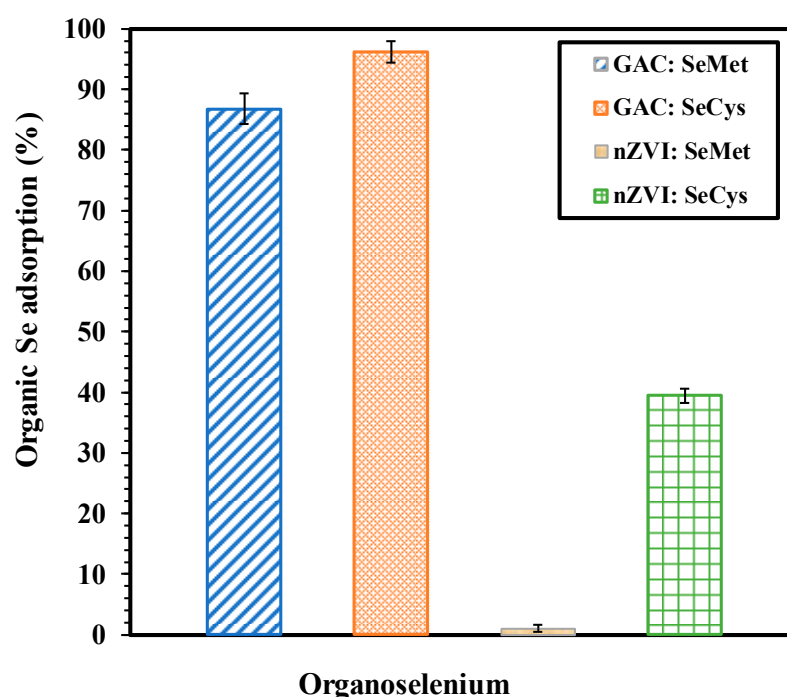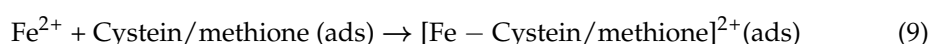

Figure 2. Comparison of organic selenium removal using 7 g/L of GAC and nZVI, pH 7.0, at 25 °C for 3 h period.

Conversely, the elemental iron (nZVI) removal mechanism for organic selenium (selenoyanate) is driven by a corrosion process, which removes the dense oxide layer and activates Fe(0) [31]. Meng [31] demonstrated that, when Fe(0) is mixed in water in the presence of dissolved oxygen (DO), Fe(0) is oxidized to ferrous ions. The oxidation process will give rise to ferric ions, which subsequently form loose ferric hydroxide in water. This phenomenon is referred to as the Fe(0) adsorption process [34], and it describes the nZVI removal mechanism of selenocyanates. In light of selenocyanate being an organic selenium compound and has similar characteristics, such as SeMet and SeCys, it is expected that a similar removal process may be applicable.

In comparison, GAC has better performance and can be attributed to the following reasons—(1) activated carbon possesses a microporous structure, which can lead to large active surface area (~1000 m^2/g) [43], with BET pore volume 0.500 (cm^3/g), and average pore width 2.138 (nm). The second reason is that activated carbon-oxygen surface functional groups (e.g., carboxylic and phenolic groups) can react with SeCys and SeMet to form chemical bonds. SeMet and SeCys are known to contain amino and a carboxylic acid; the functional groups can create hydrogen-bonding with activated carbon surface oxygen [44,45]. Additionally, selenium has an electronegativity similar to sulfur and is capable of forming strong hydrogen bonds identical to sulfur and oxygen [46].

On the other hand, nZVI adsorption was weak; it can be ascribed to the limited number of active sites. The surface area is much smaller than GAC, usually less than 100 m^2/g [47,48]. The adsorption of SeCys and SeMet on metals has not been reported in the literature. However, the mechanism can possibly be understood through the published studies on the interaction between metals, cysteine and methionine. Selenocysteine is an analogue of cysteine with selenium in place of the sulfur, while selenomethionine is analogue of methionine with selenium in place of the sulfur. Therefore, it is expected that the contaminants would have similar behavior and interactions with iron. Generally, the first steps in the adsorption of cysteine or methionine on an iron surface involve the replacement of one or more water molecules adsorbed at the iron surfaces, followed by the formation of iron-cysteine/methionine complexes, as shown in Equations (7)–(9) [49]. It is reported that cysteine can bond to the metal surface through sulfur, two oxygen, and a nitrogen atom in a four-point "quadrangular footprint", while methionine adsorbs on the surface with two oxygen and a nitrogen atom in a "triangular footprint" [50]. The sulfur atom within the methionine molecule does not interact with the metal surface. The reaction between the sulfur atom and the metal substrate can form a strong bond [50,51], indicating that cysteine's adsorption is stronger than methionine. Similar to methionine, the selenium atom in SeMet is not expected to react with iron's surface, hence no strong bond; which explains the weak adsorption of SeMet on the surface of iron compared to selenocysteine.

$$\text{Cystein/methione(sol)} + x\text{H}_2\text{O(ads)} \rightarrow \text{Cystein/methione (ads)} + x\text{H}_2\text{O(sol)} \quad (7)$$

$$\text{Fe} \rightarrow \text{Fe}^{2+} + 2e \quad (8)$$

$$\text{Fe}^{2+} + \text{Cystein/methione (ads)} \rightarrow [\text{Fe} - \text{Cystein/methione}]^{2+}\text{(ads)} \quad (9)$$

3.2. Adsorbent Dosage

Figure 3 presents the result of the adsorbent amount study on the uptake of SeMet and SeCys by GAC and nZVI with an initial concentration of 5 mg/L at pH 7.0. The removal percentage of organoselenium increased with an increase in the dose of GAC and nZVI. As shown in Figure 3, the effect of adsorbent dose on the organic selenium removal was more significant at the lower adsorbent loadings. Approximately 86.3% of SeCys and 57.1% of SeMet were removed by 1.0 g/L of GAC in 3 h. While 12.2% of SeCys was removed by nZVI within the same time frame. About 72.6% and 90% of SeMet was swiftly removed when the GAC dose was increased from 2 to 14 g/L, respectively. While 93% and 97.9% of SeCys were adsorbed from the solution with the same GAC loading. About 39.4% and

56.6% of SeCys were adsorbed by 7 and 14 g/L of nZVI, respectively. The increase in the adsorption capacity of the adsorbent candidates (GAC and nZVI) is attributed to the availability of greater surface area that drives an increase in the number of active adsorption sites; therefore, resulting in a higher removal rate [35,38]. In contrast to nZVI adsorption, an optimum dose of 7 g/L of GAC significantly adsorbed both contaminants.
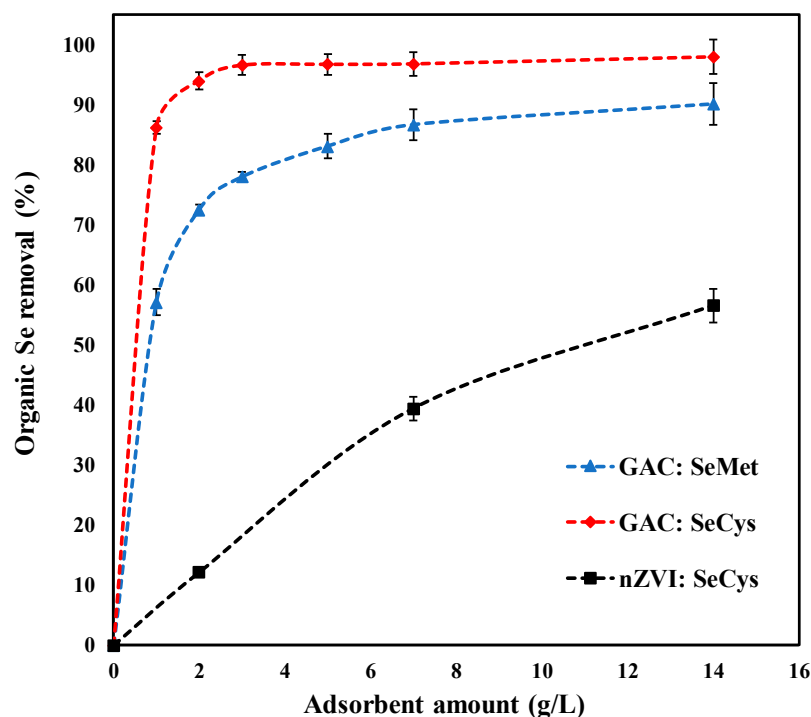

Figure 3. Effect of adsorbent dosage on organic selenium removal, by GAC and nZVI (initial concentration of 5 mg/L, pH 7.0, at 25 °C).

3.3. Effect of pH

Figure 4 depicts the results of experiments conducted to determine the pH influence on organic selenium adsorption by GAC and nZVI. The solutions pH level was measured at pH 4.0, 7.0 and 9.0 during mixing for 3 h. As shown in Figure 4, the amount of SeMet and SeCys adsorbed onto GAC for acidic, neutral and alkaline pH was significant. The removal efficiency of SeCys by GAC occurred in the order of 94.7%, 96.1% and 96.8% for pH 4.0, 7.0 and 9.0, respectively. The acidic condition was observed to be slightly less favorable for the adsorption of SeMet by GAC, corresponding to 80.3% removal. The removal of SeMet at pH 7.0 and 9.0 solution was 86.7% and 86.6%, respectively. SeCys and SeMet are zwitterions, containing both amino groups and carboxyl groups. The isoelectric point (Ip) for SeMet and SeCys are 5.75 and 5.54, respectively [51,52]. Increasing the pH from 4.0 to 9.0 would change the net charge of SeCys and SeMet solution from positive to negative and also influence the surface charge of activated carbon, leading to different electrostatic interactions between SeCys and SeMet molecules and activated carbon. In this study, the investigated pHs insignificantly impacted the adsorption of the two organic selenium compounds by GAC, indicating that the adsorption of SeCys and SeMet by GAC was not dominated by electrostatic force. The adsorption of SeCys and SeMet could potentially occur as a result of the hydrogen bonding or the hydrophobic interaction that exists between the hydrophobic part of SeCys and SeMet molecules and the hydrophobic part of the adsorbent, which have been reported as mechanisms for the adsorption of amino acids on the surface of activated carbon [53].
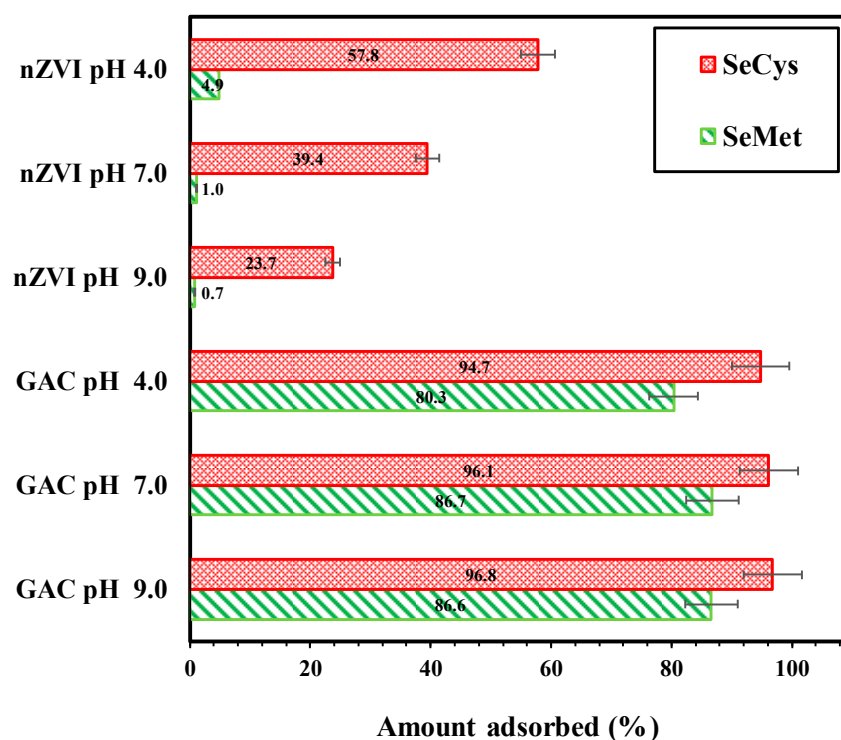
Figure 4. Effect of pH on SeMet and SeCys adsorption by GAC and nZVI, (initial concentration 5 mg/L, 7 g/L, pH 4.0, 7.0 and 9.0, at 25 °C).

On the other hand, the removal of SeCys and SeMet by nZVI decreased remarkably with increasing pH, as shown in Figure 4. The percentages of SeCys adsorbed on nZVI under different pHs are 57.8% for pH 4.0, 39.4% for pH 7.0 and 23.7% for pH 9.0. SeMet removal rate decreased from 4.9% to less than 1% when pH was increased from 4.0 to 9.0, indicating a negative effect of an increase in pH condition. Similar findings have been reported on selenocyanate adsorption (an organic selenium species) by nZVI [31]. Meng et al. [31] demonstrated that selenocyanate's removal rate increased from 50% to 97% when pH was decreased from 8.5 to 5.5.

3.4. Effect of Initial Concentration

GAC performance in treating water containing different concentrations of SeMet and SeCys at pH 7.0 is presented in Figure 5. For SeMet, 4.9 mg/L and 46.8 mg/L of initial concentration were evaluated, while SeCys, 3.8 and 38 mg/L of initial concentration were examined. Both forms of organoselenium were adsorbed continuously as a function of time until equilibrium was reached. However, SeMet appears to have some desorption after 1 h, which was typical in both concentrations (4.9 and 46.8 mg/L). The pseudo-second-order kinetic model adequately describes the data depicted in Table 2. The correlation coefficients (R^2) value was evaluated between 0.999–1.000 (Table 2). As illustrated in Table 2, the rate constant is between 2.50 to 1.80 for SeMet C_o (4.9 and 46.8 mg/L) and 1.30 to 0.25 for SeCys C_o (3.8 and 38 mg/L), respectively. The result demonstrates that the rate constant (K_2) decreased with an increase in SeMet and SeCys concentration. When the initial concentration is increased, the solution takes more time to attain equilibrium. The decrease in K_2, with respect to an increase in the initial concentration, can be attributed to a longer duration that is required for the solution to attain equilibrium; a similar phenomenon has been reported in the literature [54,55].
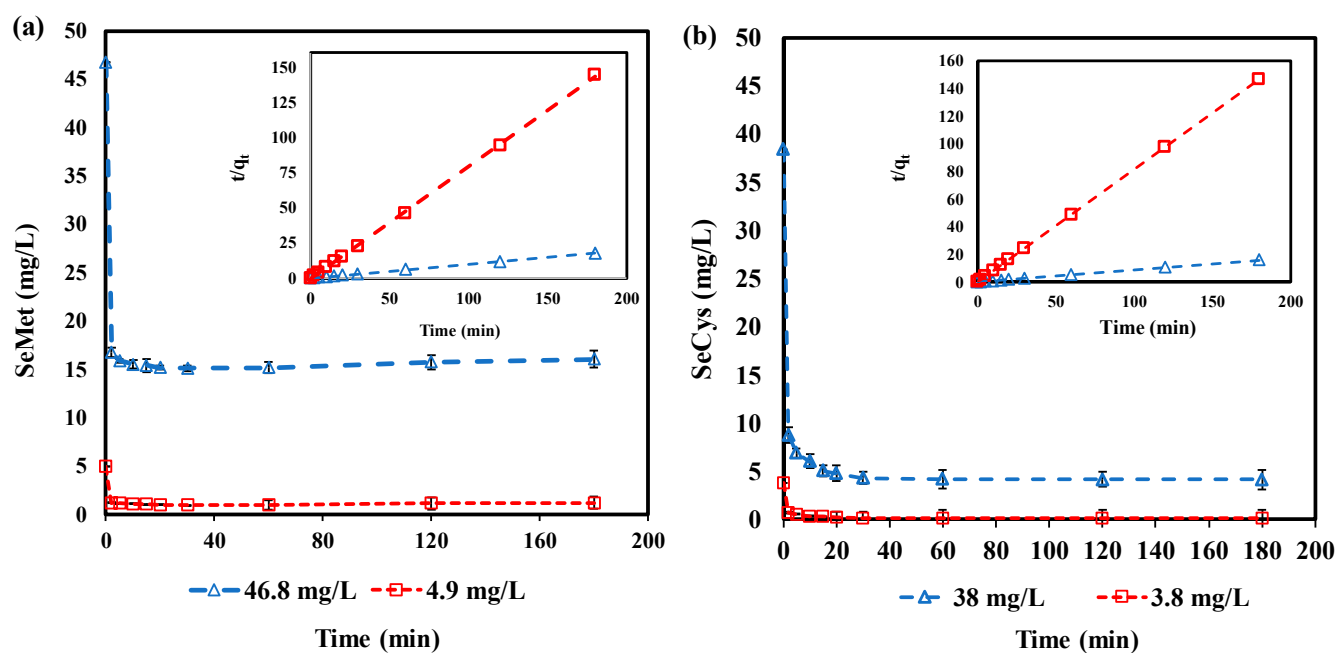
Figure 5. Effect of initial concentration by GAC: (**a**) SeMet (C_o: 46.8 and 4.9 mg/L); (**b**) SeCys (C_o: 38 and 3.8 mg/L); all experiments were conducted at pH 7.0, 7 g/L and 25 °C.

Table 2. Experimental data for adsorbate initial concentration studies with GAC adsorbent, at pH 7.0.

|	**SeMet**		**SeCys**	
C_o (mg/L)	4.9	46.8	3.8	38
q_e (mg·g^{-1})	1.32	10.54	1.23	11.40
K_2 (g·mg^{-1}·min^{-1})	2.50	1.80	1.30	0.25
R^2	1.000	0.999	1.000	1.000

Furthermore, the experimental data also show that q_e increases with higher C_o, the increment was significant about eight times higher as the initial concentrations of SeMet and SeCys were varied. It can be deduced that the increase in C_o provides the driving force to overcome the mass transfer resistance between the adsorbate and solid phases [56]. It was observed that GAC completely removed 3.8 mg/L of SeCys in 30 min, while the initial concentration of 38 mg/L was reduced to 4.2 mg/L in 3 h. About 30.7 and 3.6 mg/L of SeMet were adsorbed from the initial concentration of 46.8 and 4.9 mg/L, respectively. An upsurge in adsorption capacity as a result of an increase in adsorbate initial concentration has been reported by Aksu [57] and Al-Ghouti [58].

3.5. Adsorption Isotherm

The adsorption data for GAC were evaluated using Langmuir and Freundlich isotherm models. The results of both Langmuir and Freundlich models for SeMet and SeCys adsorption are summarized in Table 3. Freundlich and Langmuir models fitted well with the experimental data (R^2 > 0.950). Figure 6a shows that the Freundlich model provided a better fit for SeMet adsorption data compared to the Langmuir model. The correlation coefficient (R^2 > 0.996) was higher for the Freundlich model, suggesting that the adsorption of SeMet might occur in multilayers. The parameter K_f of the Freundlich model was calculated to be 1.85, which is related to the adsorption capacity. As reflected in Table 3, the constant *n*, representing the adsorption intensity, was equal to 1.55, indicating pseudo linear adsorption [59].

Table 3. Adsorption isotherm parameters for organoselenium by GAC.

	Langmuir Model			Freundlich Model		
	q_m (mg/g)	K_c (L/mg)	R^2	K_f	n	R^2
SeMet	18.9	0.10	0.967	1.85	1.55	0.996
SeCys	10.0	0.32	0.999	2.52	2.14	0.950
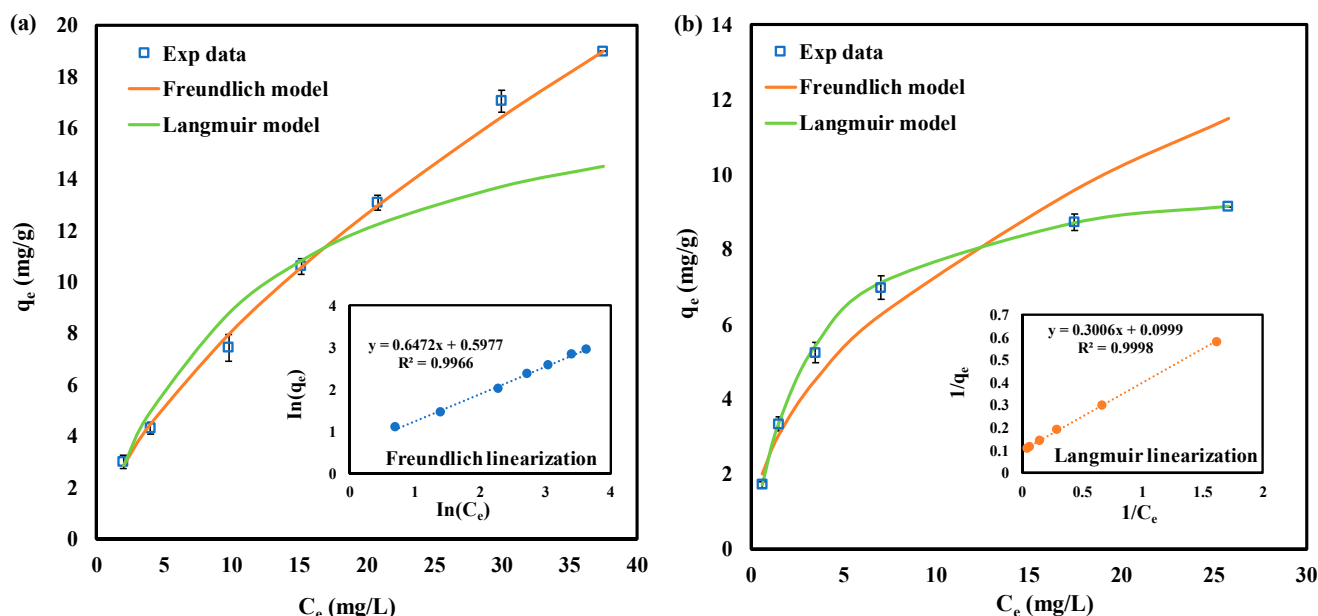
Figure 6. Organic selenium adsorption isotherms by GAC, pH 7.0, at 25 °C. (**a**) SeMet; (**b**) SeCys. The solid lines represent model fits; inset shows a linearization fit.

On the other hand, SeCys adsorption by GAC with corresponding Langmuir plots is presented in Figure 6b. Freundlich isotherm was also used to normalize the adsorption data. As stated in Table 3, the isotherm data fitted better with the Langmuir model (higher coefficients of determination R^2 = 0.990) in contrast to the Freundlich model, suggesting that the adsorption of SeCys is monolayer and it occurred at localized sites [53,57]. The maximum uptake capacity for the Langmuir parameter q_m is 10 mg/g. The dimensionless constant R_L = 0.082, an indication that SeCys adsorption process can be considered as favorable [41].

3.6. Adsorption Kinetics

Figure 7a shows the time-dependent data of SeMet and SeCys adsorption by GAC. As shown in the results (Figure 7a), the equilibrium time for SeMet was 20 min, while SeCys took longer than 50 min to achieve equilibrium, indicating that the SeCys adsorption process was progressive. The pseudo-second-order (PSO) kinetics model (inset of Figure 6a) was used to investigate the adsorption kinetics, the rate constant (k_2) values and the maximum adsorption capacity (q_e) for SeMet and SeCys, as presented in Table 4. The correlation coefficients (R^2 > 0.999) suggest that the PSO model was a good fit for the adsorbents tested. However, when parameter h, which accounts for the initial adsorption rate, was calculated, the value shows that SeCys adsorption was faster than SeMet adsorption (h value of SeMet is about 33% less than SeCys).
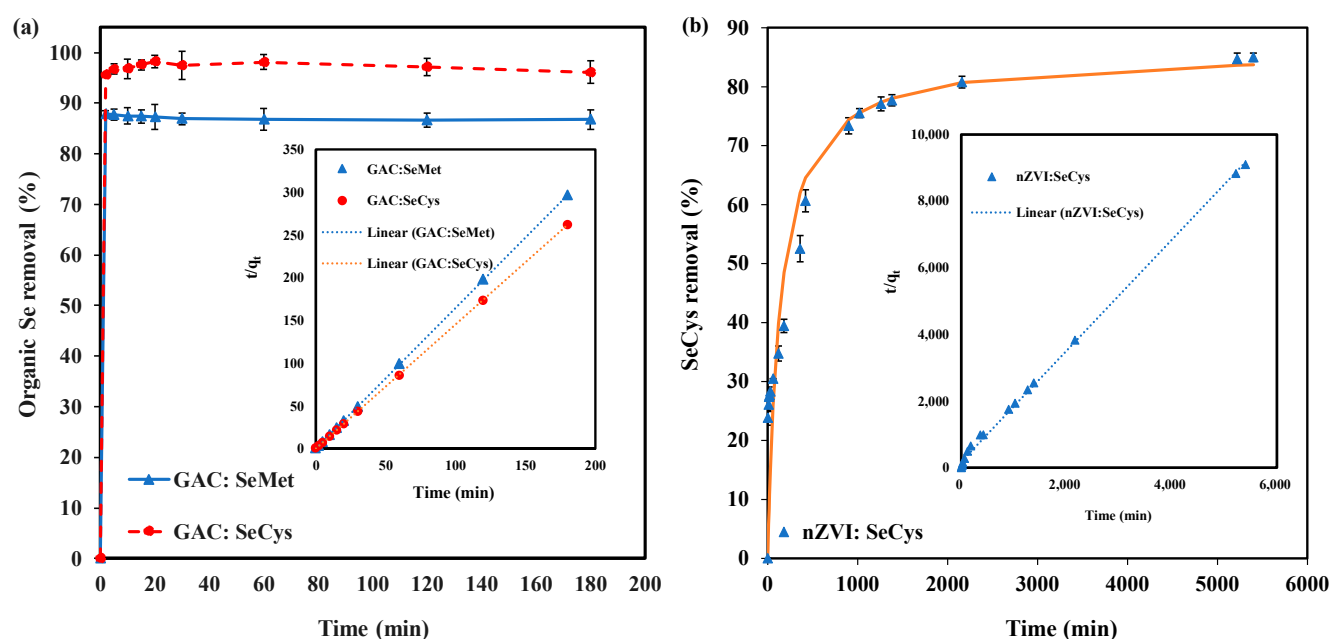
Figure 7. (**a**) Organic selenium adsorption kinetics using 7 g/L of GAC. (**b**) SeCys adsorption kinetics using 7 g/L of nZVI. All experiments were conducted at pH 7.0, 25 °C with an initial concentration of 5 mg/L.

Table 4. Kinetic parameters of pseudo-second-order models for SeMet and SeCys adsorption.

Kinetic Parameter	pH	SeMet	SeCys	
		GAC	nZVI	GAC
q_e (mg·g^{-1})		0.61	0.59	0.70
k_2 (g·mg^{-1}·min^{-1})	7	24	0.012	28
R^2		1.000	0.998	0.999
h (mg·g^{-1}·min^{-1})		8.81	0.004	13.27

The adsorption kinetics of SeCys by nZVI are depicted in Figure 7b. The experiment was performed for 54 h to allow enough time for equilibrium. However, equilibrium was not achieved because the adsorption process was very slow (Table 4). The pseudo-second-order kinetics model showed a good fit for SeCys adsorption data ($R^2 > 0.998$). Contrary to GAC adsorption, nZVI removal efficiency was found to increase slowly until a final adsorption efficiency of 85% was achieved. Overall, GAC kinetics was very swift compared to nZVI, which can be explained as an outcome of a more significant adsorption site [43].

3.7. Binary Adsorption of SeMet and SeCys

The effect of the coexistence of SeMet and SeCys on wastewaters was investigated using 7 g/L of GAC and nZVI. The initial concentration of organic selenium in the mixture was 10 mg/L (comprising 5 mg/L of SeMet and SeCys each), and the pH of the solution was 7.0. The result presented in Figure 8 shows that GAC and nZVI removed 8.9 mg/L and 1.5 mg/L of Se from the mixture of SeMet and SeCys, respectively, in 3 h. On an individual basis, GAC removed 4.8 mg/L of Se from SeCys solution and 4.3 mg/L of Se from SeMet solution. While nZVI adsorbed 1.9 mg/L of Se from SeCys and 0.1 mg/L of Se from SeMet. The result shows that the total Se removed by GAC from the mixture of SeMet and SeCys solution was lower compared to the sum of Se adsorbed in a single solute system. This phenomenon is an indication of competition between different molecules for available adsorption sites on GAC surface [60,61]. Conversely, the adsorption of SeMet by nZVI in a single solute system was very weak, indicating that the competing effect for active sites on the surface of nZVI was negligible. The inhibition effect of SeMet on the adsorption of

SeCys by GAC and nZVI can possibly occur as a result of the interaction between SeCys and SeMet in the binary system. Organic selenium speciation was not determined in this study; hence, the selenium species removed from the mixture was unknown.
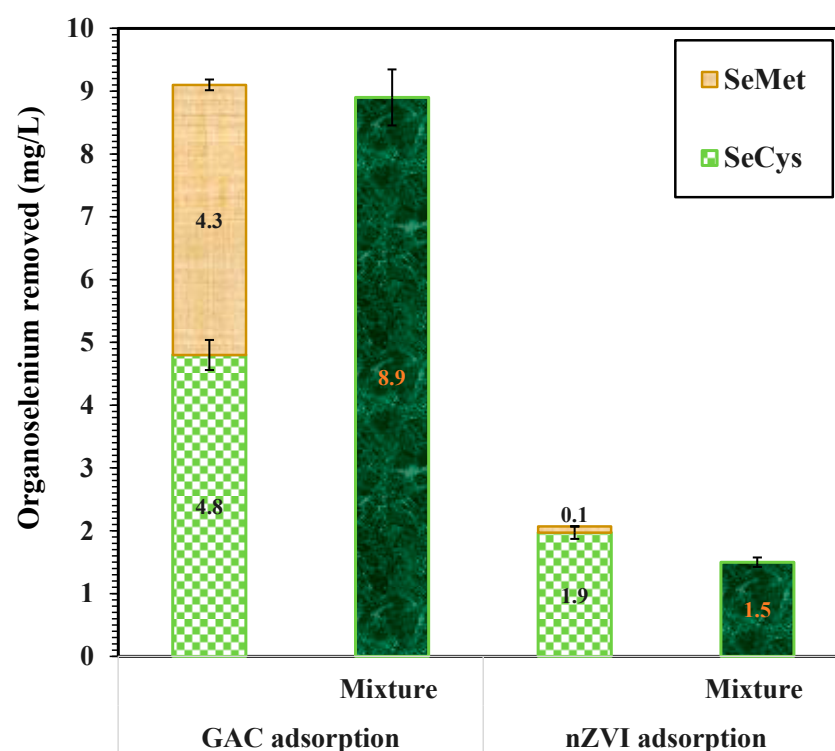

Figure 8. Binary adsorption of SeMet and SeCys by nZVI and GAC, initial concentration of 10 mg/L, 7 g/L at pH 7.0 and 25 °C.

4. Conclusions

The adsorption of SeMet and SeCys by GAC and nZVI under various conditions—different pHs, adsorbate initial concentration, adsorbent dosage, and binary adsorption were investigated. GAC demonstrated a higher affinity towards the removal of SeMet and SeCys, and was, therefore, considered a better adsorbent candidate. An optimum dose of 7 g/L of GAC was found to remove both contaminants effectively. Change in pH had no significant impact on SeCys removal by GAC; nevertheless, more than 93.99% removal was achieved at all pH tested. In the case of nZVI, pH change substantially influenced the adsorption capacity—at pH 4.0, about 57.8% of SeCys was removed. An increase in adsorption capacity with a decrease in pH value was observed for SeMet removal by nZVI. SeCys adsorbed more readily into nZVI compared to SeMet—for all conditions evaluated, SeMet removal by nZVI was less than 5%. The pseudo-second-order kinetics model characterized the adsorption of organoselenium by both adsorbents. The fastest adsorption kinetics was observed with GAC under neutral pH, where an instantaneous removal of organic selenium was observed. Binary adsorption of SeCys and SeMet indicates an inhibitory effect on SeCys removal by SeMet. The adsorption data fitted well with both Langmuir and Freundlich isotherm models.

References

1.　Maseko, T.; Callahan, D.L.; Dunshea, F.R.; Doronila, A.; Kolev, S.D.; Ng, K. Chemical characterisation and speciation of organic selenium in cultivated selenium-enriched Agaricus bisporus. *Food Chem.* **2013**, *141*, 3681–3687. [CrossRef] [PubMed]

2.　Dumont, E.; Vanhaecke, F.; Cornelis, R. Selenium speciation from food source to metabolites: A critical review. *Anal. Bioanal. Chem.* **2006**, *385*, 1304–1323. [CrossRef] [PubMed]

3.　Amoako, P.O.; Uden, P.C.; Tyson, J.F. Speciation of selenium dietary supplements; formation of S-(methylseleno) cysteine and other selenium compounds. *Anal. Chim. Acta* **2009**, *652*, 315–323. [CrossRef] [PubMed]

4.　Albert, M.; Demesmay, C.; Rocca, J. Analysis of organic and non-organic arsenious or selenious compounds by capillary electrophoresis. *Fresenius' J. Anal. Chem.* **1995**, *351*, 426–432. [CrossRef]

5.　LeBlanc, K.L.; Wallschläger, D. Production and release of selenomethionine and related organic selenium species by microorganisms in natural and industrial waters. *Environ. Sci. Technol.* **2016**, *50*, 6164–6171. [CrossRef] [PubMed]

6.　Lemly, A.D. Environmental implications of excessive selenium: A review. *Biomed. Environ. Sci.* **1997**, *10*, 415–435.

7.　Fan, A.M.; Book, S.A.; Neutra, R.R.; Epstein, D.M. Selenium and human health implications in California's San Joaquin Valley. *J. Toxicol. Environ. Health Part A Curr. Issues* **1988**, *23*, 539–559. [CrossRef]

8.　Delos, C. *Draft Aquatic Life Water Quality Criteria for Selenium*; US Environmental Protection Agency: Washington, DC, USA, 2004.

9.　CH2M HILL. Review of available technologies for the removal of selenium from water. In *Final Report, Prepared for North American Metals Council (NAMC)*; CH2M HILL: Charlotte, NC, USA; Bellevue, WA, USA, 2010.

10.　Khamkhash, A.; Srivastava, V.; Ghosh, T.; Akdogan, G.; Ganguli, R.; Aggarwal, S. Mining-related selenium contamination in Alaska, and the state of current knowledge. *Minerals* **2017**, *7*, 46. [CrossRef]

11.　Zhang, Y.; Amrhein, C.; Frankenberger, W.T., Jr. Effect of arsenate and molybdate on removal of selenate from an aqueous solution by zero-valent iron. *Sci. Total Environ.* **2005**, *350*, 1–11. [CrossRef]

12.　Mondal, K.; Jegadeesan, G.; Lalvani, S.B. Removal of selenate by Fe and NiFe nanosized particles. *Ind. Eng. Chem. Res.* **2004**, *43*, 4922–4934. [CrossRef]

13.　Montgomery, J.M.; Engineers, C. *Water Treatment Principles and Design*; Wiley: New York, NY, USA, 1985.

14.　Mavrov, V.; Stamenov, S.; Todorova, E.; Chmiel, H.; Erwe, T. New hybrid electrocoagulation membrane process for removing selenium from industrial wastewater. *Desalination* **2006**, *201*, 290–296. [CrossRef]

15.　Balistrieri, L.S.; Chao, T. Selenium Adsorption by Goethite. *Soil Sci. Soc. Am. J.* **1987**, *51*, 1145–1151. [CrossRef]

16.　Balistrieri, L.S.; Chao, T. Adsorption of selenium by amorphous iron oxyhydroxide and manganese dioxide. *Geochim. Cosmochim. Acta* **1990**, *54*, 739–751. [CrossRef]

17.　Zhang, Y.; Frankenberger, W.T. Factors affecting removal of selenate in agricultural drainage water utilizing rice straw. *Sci. Total Environ.* **2003**, *305*, 207–216. [CrossRef]

18.　Peak, D. Adsorption mechanisms of selenium oxyanions at the aluminum oxide/water interface. *J. Colloid Interface Sci.* **2006**, *303*, 337–345. [CrossRef]

19.　El-Shafey, E. Sorption of Cd (II) and Se (IV) from aqueous solution using modified rice husk. *J. Hazard. Mater.* **2007**, *147*, 546–555. [CrossRef]

20.　Zhang, N.; Gang, D.; Lin, L.-S. Adsorptive removal of parts per million level Selenate using iron-coated GAC Adsorbents. *J. Environ. Eng.* **2010**, *136*, 1089–1095. [CrossRef]

21.　Zhang, N.; Lin, L.-S.; Gang, D. Adsorptive selenite removal from water using iron-coated GAC adsorbents. *Water Res.* **2008**, *42*, 3809–3816. [CrossRef]

22.　Hu, C.; Chen, Q.; Chen, G.; Liu, H.; Qu, J. Removal of Se (IV) and Se (VI) from drinking water by coagulation. *Sep. Purif. Technol.* **2015**, *142*, 65–70. [CrossRef]

23.　Tan, T.; Beydoun, D.; Amal, R. Effects of organic hole scavengers on the photocatalytic reduction of selenium anions. *J. Photochem. Photobiol. A Chem.* **2003**, *159*, 273–280. [CrossRef]

24.　Nguyen, V.N.H.; Beydoun, D.; Amal, R. Photocatalytic reduction of selenite and selenate using TiO$_2$ photocatalyst. *J. Photochem. Photobiol. A Chem.* **2005**, *171*, 113–120. [CrossRef]

25.　Zhang, Y.; Moore, J.N. Environmental conditions controlling selenium volatilization from a wetland system. *Environ. Sci. Technol.* **1997**, *31*, 511–517. [CrossRef]

26.　Amweg, E.; Stuart, D.; Weston, D. Comparative bioavailability of selenium to aquatic organisms after biological treatment of agricultural drainage water. *Aquat. Toxicol.* **2003**, *63*, 13–25. [CrossRef]

27.　Zhang, Y.; Okeke, B.C.; Frankenberger, W.T., Jr. Bacterial reduction of selenate to elemental selenium utilizing molasses as a carbon source. *Bioresour. Technol.* **2008**, *99*, 1267–1273. [CrossRef] [PubMed]

28. Presser, T.S.; Ohlendorf, H.M. Biogeochemical cycling of selenium in the San Joaquin Valley, California, USA. *Environ. Manag.* **1987**, *11*, 805–821. [CrossRef]

29. Ohlendorf, H.M. Bioaccumulation and Effects of Selenium in Wildlife. *Selenium Agric. Environ.* **1989**, *23*, 133–177.

30. Manceau, A.; Gallup, D.L. Removal of Selenocyanate in Water by Precipitation: Characterization of Copper−Selenium Precipitate by X-ray Diffraction, Infrared, and X-ray Absorption Spectroscopy. *Environ. Sci. Technol.* **1997**, *31*, 968–976. [CrossRef]

31. Meng, X.; Bang, S.; Korfiatis, G.P. Removal of selenocyanate from water using elemental iron. *Water Res.* **2002**, *36*, 3867–3873. [CrossRef]

32. Latva, S.; Peräniemi, S.; Ahlgrén, M. Study of metal-loaded activated charcoals for the separation and determination of selenium species by energy dispersive X-ray fluorescence analysis. *Anal. Chim. Acta* **2003**, *478*, 229–235. [CrossRef]

33. Okonji, S.O.; Dominic, J.A.; Pernitsky, D.; Achari, G. Removal and recovery of selenium species from wastewater: Adsorption kinetics and co-precipitation mechanisms. *J. Water Process Eng.* **2020**, *38*, 101666. [CrossRef]

34. Yoon, I.-H.; Kim, K.-W.; Bang, S.; Kim, M.G. Reduction and adsorption mechanisms of selenate by zero-valent iron and related iron corrosion. *Appl. Catal. B Environ.* **2011**, *104*, 185–192. [CrossRef]

35. Wasewar, K.L.; Prasad, B.; Gulipalli, S. Removal of selenium by adsorption onto granular activated carbon (GAC) and powdered activated carbon (PAC). *CLEAN–Soil Air Water* **2009**, *37*, 872–883. [CrossRef]

36. Das, S.; Lindsay, M.B.; Essilfie-Dughan, J.; Hendry, M.J. Dissolved selenium (VI) removal by zero-valent iron under oxic conditions: Influence of sulfate and nitrate. *ACS Omega* **2017**, *24*, 1513–1522. [CrossRef] [PubMed]

37. Zhang, Y.; Wang, J.; Amrhein, C.; Frankenberger, W.T. Removal of selenate from water by zerovalent iron. *J. Environ. Qual.* **2005**, *34*, 487–495. [CrossRef] [PubMed]

38. Liang, L.; Jiang, X.; Yang, W.; Huang, Y.; Guan, X.; Li, L. Kinetics of selenite reduction by zero-valent iron. *Desalination Water Treat.* **2015**, *53*, 2540–2548. [CrossRef]

39. Zelmanov, G.; Semiat, R. Selenium removal from water and its recovery using iron (Fe3+) oxide/hydroxide-based nanoparticles sol (NanoFe) as an adsorbent. *Sep. Purif. Technol.* **2013**, *103*, 167–172. [CrossRef]

40. Langmuir, I. The constitution and fundamental properties of solids and liquids. Part I. Solids. *J. Am. Chem. Soc.* **1916**, *38*, 2221–2295. [CrossRef]

41. Zeng, G.; Liu, Y.; Tang, L.; Yang, G.; Pang, Y.; Zhang, Y.; Zhou, Y.; Li, Z.; Li, M.; Lai, M. Enhancement of Cd (II) adsorption by polyacrylic acid modified magnetic mesoporous carbon. *Chem. Eng. J.* **2015**, *259*, 153–160. [CrossRef]

42. Bansal, R.; Goyal, M. Activated carbon adsorption and environment: Adsorptive removal of organic from water. In *Activated Carbon Adsorption*; Taylor & Francis: Boca Raton, FL, USA, 2005; pp. 297–372.

43. Yang, Y.; Yu, L.; Iranmanesh, S.; Keir, I.; Achari, G. Laboratory and Field Investigation of Sulfolane Removal from Water Using Activated Carbon. *J. Environ. Eng.* **2020**, *146*, 04020022. [CrossRef]

44. Ahnert, F.; Arafat, H.A.; Pinto, N.G. A study of the influence of hydrophobicity of activated carbon on the adsorption equilibrium of aromatics in non-aqueous media. *Adsorption* **2003**, *9*, 311–319. [CrossRef]

45. López-Velandia, C.; Moreno-Barbosa, J.J.; Sierra-Ramirez, R.; Giraldo, L.; Moreno-Piraján, J.C. Adsorption of volatile carboxylic acids on activated carbon synthesized from watermelon shells. *Adsorpt. Sci. Technol.* **2014**, *32*, 227–242. [CrossRef]

46. Mundlapati, V.R.; Sahoo, D.K.; Ghosh, S.; Purame, U.K.; Pandey, S.; Acharya, R.; Pal, N.; Tiwari, P.; Biswal, H.S. Spectroscopic evidence for strong hydrogen bonds with selenomethionine in proteins. *J. Phys. Chem. Lett.* **2017**, *8*, 794–800. [CrossRef] [PubMed]

47. Adusei-Gyamfi, J.; Acha, V. Carriers for nano zerovalent iron (nZVI): Synthesis, application and efficiency. *RSC Adv.* **2016**, *6*, 91025–91044. [CrossRef]

48. Wang, Q.; Kanel, S.R.; Park, H.; Ryu, A.; Choi, H. Controllable synthesis, characterization, and magnetic properties of nanoscale zerovalent iron with specific high Brunauer–Emmett–Teller surface area. *J. Nanoparticle Res.* **2009**, *113*, 749–755. [CrossRef]

49. Oguzie, E.; Li, Y.; Wang, F. Corrosion inhibition and adsorption behavior of methionine on mild steel in sulfuric acid and synergistic effect of iodide ion. *J. Colloid Interface Sci.* **2007**, *310*, 90–98. [CrossRef] [PubMed]

50. Thomsen, L.; Wharmby, M.; Riley, D.; Held, G.; Gladys, M. The adsorption and stability of sulfur containing amino acids on Cu {5 3 1}. *Surf. Sci.* **2009**, *603*, 1253–1261. [CrossRef]

51. Mishra, B.; Priyadarsini, K.; Mohan, H. One-Electron Oxidation of Selenomethionine in Aqueous Solutions. *Barc Newslett.* **2005**, *261*, 115.

52. Bettelheim, F.A.; Brown, W.H.; Campbell, M.K.; Farrell, S.O.; Torres, O. *Introduction to General, Organic and Biochemistry*; Nelson Education: Toronto, ON, Canada, 2012.

53. Cermakova, L.; Kopecka, I.; Pivokonsky, M.; Pivokonska, L.; Janda, V. Removal of cyanobacterial amino acids in water treatment by activated carbon adsorption. *Sep. Purif. Technol.* **2017**, *173*, 330–338. [CrossRef]

54. Gupta, S.S.; Bhattacharyya, K.G. Kinetics of adsorption of metal ions on inorganic materials: A review. *Adv. Colloid Interface Sci.* **2011**, *162*, 39–58. [CrossRef]

55. Allen, S.J.; Gan, Q.; Matthews, R.; Johnson, P.A. Kinetic modeling of the adsorption of basic dyes by kudzu. *J. Colloid Interface Sci.* **2005**, *286*, 101–109. [CrossRef]

56. Wang, W.; Wang, J.; Guo, Y.; Zhu, C.; Pan, F.; Wu, R.; Wang, C. Removal of multiple nitrosamines from aqueous solution by nanoscale zero-valent iron supported on granular activated carbon: Influencing factors and reaction mechanism. *Sci. Total Environ.* **2018**, *639*, 934–943. [CrossRef] [PubMed]

57. Aksu, Z.; Dönmez, G. A comparative study on the biosorption characteristics of some yeasts for Remazol Blue reactive dye. *Chemosphere* **2003**, *50*, 1075–1083. [CrossRef]

58. Al-Ghouti, M.A.; Khraisheh, M.A.; Ahmad, M.N.; Allen, S. Adsorption behaviour of methylene blue onto Jordanian diatomite: A kinetic study. *J. Hazard. Mater.* **2009**, *165*, 589–598. [CrossRef] [PubMed]

59. Tseng, R.-L.; Wu, F.-C. Inferring the favorable adsorption level and the concurrent multi-stage process with the Freundlich constant. *J. Hazard. Mater.* **2008**, *155*, 277–287. [CrossRef]

60. Jain, J.S.; Snoeyink, V.L. Adsorption from bisolute systems on active carbon. *J. Water Pollut. Control Fed.* **1973**, *45*, 2463–2479.

61. Noroozi, B.; Sorial, G.; Bahrami, H.; Arami, M. Adsorption of binary mixtures of cationic dyes. *Dyes Pigment.* **2008**, *76*, 784–791. [CrossRef]